치의학 박사학위논문

Effects of Miniscrew-Assisted Rapid Palatal Expansion on Airflow in the Upper Airway of an Adult Patient with Obstructive Sleep Apnea Syndrome: Computational Simulation using Fluid-Structure Interaction

미니스크류를 이용한 급속구개확장술이 폐쇄성 수면무호흡증이 있는 성인 환자의 상기도 호흡에 미치는 영향: 유체구조연계 분석법

2017년 8월

서울대학교 대학원

치의학과 치과교정학 전공

허 재 식

Effects of Miniscrew-Assisted Rapid Palatal Expansion on Airflow in the Upper Airway of an Adult Patient with Obstructive Sleep Apnea Syndrome: Computational Simulation using Fluid-Structure Interaction

지도교수 백 승 학

이 논문을 치의학 박사학위논문으로 제출함.
2017년 4월

서울대학교 대학원
치의학과 치과교정학 전공

허 재 식

허재식의 박사학위논문을 인준함.
2017년 6월

위 원 장 (인)

부위원장 (인)

위 원 (인)

위 원 (인)

위 원 (인)

ABSTRACT

Effects of Miniscrew-Assisted Rapid Palatal Expansion on Airflow in the Upper Airway of an Adult Patient with Obstructive Sleep Apnea Syndrome: Computational Simulation using Fluid-Structure Interaction

Jae Sik Hur, DDS, MSD

Department of Orthodontics, School of Dentistry,

Seoul National University

(Directed by Professor **Seung-Hak Baek,** DDS, MSD, PhD)

The purpose of this study was to investigate the effects of miniscrew-assisted rapid palatal expansion (MARPE) on changes in airflow in the upper airway (UA) of an adult patient with obstructive sleep apnea syndrome (OSAS).

Three-dimensional (3D) UA models of a young adult male patient with OSAS [age of 18 years and 7 months, body mass index (BMI), 25.0 kg/m^2; apnea and hypopnea index (AHI), 49.5 events/hour; respiratory disturbance index (RDI), 52.2 events/hour; lowest O_2 saturation rate (LSR), 85%] were fabricated using cone-beam computed tomography images taken before (T0) and after MARPE treatment (T1). The signs [age of 19 years and 1 month, BMI, 24.9 kg/m^2; AHI, 2.2 events/hour; RDI, 20.2 events/hour; LSR, 95%] and symptoms at the T1 stage significantly improved. A total of sixteen cross-sectional planes were set with the inter-plane distance of 10 mm along the upper airway: 7 planes for the nasal cavity and 9 planes for the pharynx. Using 3D computational fluid dynamics (3D-CFD)

and fluid-structure interaction (FSI) analysis, changes in the cross-sectional area (CSA), velocity and pressure of airflow, displacements of nodes, and total resistance were investigated at maximum inspiration (MI), rest, and maximum expiration (ME).

Compared to the T0 stage, the T1 stage exhibited significant increase in CSA at the most of parts of the nasal cavity and at the upper part of pharynx. Velocity of airflow was decreased primarily in the anterior part of the nasal cavity at MI and ME, and in the upper and middle parts of the pharynx at MI. However, the amounts of decrease were greater in the nasal cavity than the pharynx. Pressure of airflow was decreased mainly in the anterior parts of the nasal cavity and consistently in the whole pharynx. In terms of node displacement, the amount of displacement was insignificant at both T0 and T1 stages. In aspects of total resistance, there was significant decrease in the absolute values at MI (-55.1%), rest (-35.9%) and ME (-33.9 %) during T0-T1.

Since MARPE improved airflow and reduced resistance in the UA, it might be an effective treatment modality for adult OSAS patients who have moderate to severe narrow basal arch and crowding and refuse to the oral appliance or MMA surgery.

Key words: Miniscrew-assisted rapid palatal expansion; upper airway; obstructive sleep apnea syndrome; computational fluid dynamics; fluid-structure Interaction

Student Number: 2003-31129

국문초록

미니스크류를 이용한 급속구개확장술이 폐쇄성 수면무호흡증이 있는 성인 환자의 상기도 호흡에 미치는 영향: 유체구조연계 분석법

허 재 식

서울대학교 대학원 치의학과 치과교정학 전공
(지도교수 백 승 학)

본 연구는 미니스크류를 이용한 급속구개확장술이 폐쇄성 수면무호흡증이 있는 성인 환자의 상기도 호흡에 미치는 영향을 규명하기 위함을 목적으로 한다.

연구대상으로 폐쇄성 수면무호흡증이 있는 성인 남자 환자 (치료 전, 18 세 7 개월, 신체질량지수 25.0 Kg/m^2, 무호흡-저호흡지수 49.5 회/시간, 호흡 장애지수 52.2 회/시간, 최저산소포화도 85%; 치료 후, 19 세 1 개월, 신체질량지수 24.9 Kg/m^2, 무호흡-저호흡지수 2.2 회/시간, 호흡장애지수 20.2 회/시간, 최저산소포화도 95%)의 급속구개확장술 전후 촬영한 컴퓨터 단층촬영 영상을 이용하여 삼차원 상기도 모형을 제작하였다.

삼차원 상기도 모형의 비강과 인두부위에 각각 7개, 9개의 단면 (단면 간 거리 10mm) 을 모형 상에 설정하였다. 이후, 유체구조연계해석을 이용한 전산유체역학분석을 시행하여 각 단면적에서의 면적, 상기도 호흡 기류의 속도, 압력, 노드 변위량 및 전체 저항값을 최대흡기, 휴지기, 최대호기 상에서 각각 측정하였다. 급속구개확장술 전후의 각 계측값을 비교하여 다음과 같은 결과를 도출하였다.

(1) 각 단면의 면적은 비강부위와 인두의 상부에서 유의성 있는 증가량을 보였다.

(2) 기류의 속도는 최대흡기와 최대호기 시 비강의 전방부 및 인두의 상부와 중간부위에서 주로 감소하였다. 감소량의 절대치는 인두부위에 비해 비강에서 큰 값을 보였다.

(3) 압력은 주로 비강의 전방부에서 큰 감소를 보였고, 비강의 나머지 부위와 인두부는 그보다 작으며 비교적 일정한 감소를 보였다.

(4) 연조직 변위를 계산하는 노드의 변위량은 크지 않았다.

(5) 상기도의 전체 저항값은 최대흡기 시 55.1%, 휴지기 시 35.9%, 최대호기 시 33.9%가 감소하였다.

결론적으로 중등도 이상의 협소한 상악 기저골과 치열의 크라우딩 (crowding)을 보이는 폐쇄성 수면무호흡증 환자에게 미니스크류를 이용한 급속구개확장술이 하나의 치료 방법이 될 수 있음을 시사한다.

주요어 : 급속구개확장술, 상기도, 수면무호흡증, 전산유체역학,

유체구조연계 해석

학 번 : 2003-31129

Effects of Miniscrew-Assisted Rapid Palatal Expansion on Airflow in the Upper Airway of an Adult Patient with Obstructive Sleep Apnea Syndrome: Computational Simulation using Fluid-Structure Interaction

Jae Sik Hur, DDS, MSD

Department of Orthodontics, School of Dentistry,

Seoul National University

(Directed by Professor **Seung-Hak Baek,** *DDS, MSD, PhD)*

- Contents –

I. Introduction

Obstructive sleep apnea syndrome (OSAS) is characterized by a temporary cessation of breathing (apnea) or shallow breathing (hypopnea) with reduced hemoglobin oxygen saturation.[1] Clinically significant OSAS occurs in 2% to 4% of the population and is strongly correlated with obesity and age.[2] Based on the etiology, severity, and collapse site in the upper airway, various treatment modalities have been applied to OSAS patients such as weight reduction, continuous positive airway pressure device, intraoral appliance, soft tissue procedure, and maxilla-mandibular advancement (MMA) surgery.[1,3,4]

Although conventional rapid palatal expansion (RPE) with tooth-borne anchorage has been suggested as one treatment option for OSAS, the subjects of most previous studies were children patients.[5-7] Because the conventional RPE is thought to be less effective for adult patients, use of surgery-assisted RPE (SARPE) is recommended in adult OSAS patients.[8-10] However, it has some disadvantages, including surgical invasiveness and long retention period. Recently, miniscrew-assisted RPE (MARPE) is getting attention by clinicians due to its increased orthopedic effect on expansion of the maxillary basal arch width compared to conventional RPE as well as non-invasive expansion of the mid-palatal suture of adult patients compared to SARPE.[11-13] Although MARPE is thought to be helpful for relieving symptoms of OSAS,[14] there is little scientific evidence available on this topic.

Two-dimensional (2D) lateral cephalograms have served as the traditional radiographic standard for airway assessment.[15] Although 2D lateral cephalograms are considered cost-effective and less invasive, they cannot accurately depict the three-dimensional (3D) airway anatomy, especially in the axial plane, which

includes the most physiologically relevant information and is perpendicular to the direction of airflow.[16] Recently, 3D computed tomography (3D-CT) analysis has become a focus of attention for accurate evaluation of the 3D airway anatomy.[17,18,19,20,21]

Three-dimensional computational fluid dynamics (3D-CFD) has been used to investigate airflow dynamics in OSAS patients.[4,22-26] However, since the upper airway, especially the pharynx, is a deformable structure, adoption of the fluid structure interaction (FSI), which is a computational method to simulate the flow and structural changes, is recommended.[23,24] Use of an FSI simulation can overcome the limitations of the rigid wall design in CFD and produce more realistic results than CFD.[23,27]

Despite the important anatomical and physiological roles of the nasal cavity in respiration, most numerical airflow simulation studies have omitted the nasal cavity in fabrication of the 3D airway model due to the complex structure and diverse shape of the nasal cavity as well as the computational cost of airflow simulation.[22-26] To investigate the effect of MARPE on the airflow dynamics of the upper airway, the nasal cavity must be included in 3D-computational modeling and FSI analysis.[28,29] Therefore, the purpose of this study was to investigate the effects of MARPE on airflow in the upper airway of an adult OSAS patient using 3D-CFD/FSI analysis.

II. REVIEW OF LITERATURE

1. Obstructive sleep apnea syndrome

OSAS is diagnosed under following conditions: (1) during seven hours of nocturnal sleep, at least 30 apneic episodes are observed both in rapid eye movement (REM) and non-rapid eye movement (NREM) sleep; and (2) some portion of apneic episodes must appear in a repetitive sequence in NREM sleep.[30]

OSAS is known to be occurred at 5% to 15% of middle-aged working adults in the general population.[1,2,31,32] Since OSAS leads to intermittent arousals and nocturnal hypoxemia, it can cause excessive daytime sleepiness, loss of concentration, hypertension, and numerous detrimental conditions such as cardiac arrhythmias, cardiac arrest, sudden death, systemic inflammation, and endothelial dysfunctions.[33]

Although the etiology and pathogenesis of OSAS are not completely understood, anatomic obstruction and increased resistance in the postero-superior airway are known to cause OSAS.[4] The causes of OSAS are anatomical and non-anatomical factors. The airway anatomy was reported to explain 34% of the variability of OSAS severity.[34] Schwab et al.[35] insisted that the subjects with OSAS had a smaller airway cross-sectional area than normal subjects. In addition, non-anatomic factors, such as soft tissue compliance and reduced intraluminal pressure in the upper airway during inspiration, may play crucial roles in the airway obstruction and pathogenesis of OSAS.[36,37]

2. Treatment modalities of OSAS

There are various treatment options for patients with OSAS including non-surgical and surgical approaches.[1] Among non-surgical approaches, use of continuous positive airway pressure (CPAP) appliance is still the main treatment strategy for patients with OSAS. Giles et al.[38] in their Cochrane systematic review, concluded that CPAP is effective in reducing symptoms of sleepiness and improving the quality of life in patients with moderate and severe OSAS. However, the compliance to CPAP appliance is less than 50%, which is related to tolerance problems and psychological issues such as disturbances to the sleeping partners and sexual life.[39,40]

In the last decade, a variety of dental devices have been developed for treatment of OSA. Oral appliances may be attractive for OSA patients who do not satisfy with other therapies or surgical procedures.[41] Due to their reversibility, cost effectiveness, and less side effects and complications, oral appliances, despite of a lower rate of AHI reduction, can be an effective alternative to nasal CPAP.[41]

Surgical procedures in the soft and hard tissues are performed to increase the posterior airway space. Three major categories of UA surgery can be discerned: soft tissue surgery, skeletal framework surgery and tracheotomy. Soft tissue surgery aims to remove or reduce the volume of UA soft tissues such as the tonsils, uvula and soft palate or tongue base. The goal of skeletal framework surgery is to modify the facial skeleton from which the soft tis- sues are suspended. This results in a repositioning of UA soft tissues. Tracheotomy restores UA patency through bypassing the UA. In terms of the soft tissue surgery, uvulopalatopharyngoplasty(UPPP), genioglossus advancement, and tongue base reduction have been commonly performed.[42] However, although the success rate is known to be around 40% to 60%, these procedures can cause significant post-operative pain.[43]

In a recent systematic review, maxillomandibular advancement (MMA)

surgery is known to be safe and highly effective in reduction of the apnea–hypopnea index(AHI).[44] Kim et al[4] concluded that MMA could enlarge the upper airways three-dimensionally by expanding the whole skeletal framework. Tsui et al.[45] suggested that MMA might maintain or even improve the dental occlusion and masticatory function as well as make the pharyngeal soft tissues and tongue more resistant to collapse during inspiration.

3. Conventional rapid palatal expansion

In children, conventional RPE appliance can apply the orthopedic force to the midpalatal suture using tooth-born anchorage.[46] According to Camacho et al.[47] there are only two systematic reviews that evaluated the effect of conventional RPE on treatment for pediatric OSAS patients.[48,49]

However, these two well-performed studies[48,49] had several limitations as follows: 1) systematic review of non-English language studies; 2) updated AHI and oxygen saturation values (e.g., lowest oxygen saturation [LSAT]), 3) updated mean differences and standardized mean differences, 4) overall percentage change in AHI and LSAT, and 5) evaluation of the variables affecting the success of RPE.[47]

4. Surgically-assisted RPE and miniscrew-assisted RPE for OSAS

Conventional RPE is recommended only for individuals who are still growing. Once the midpalatal suture is fused, surgical osteotomies to the midpalatal suture and the buccal cortical plates of the maxilla and subsequent activation of RPE appliance are required to expand the bone segments. This method was defined as

surgically-assisted RPE (SARPE).[50] Koudstaal et al.[51] suggested that SARPE is an effective technique for treating maxillary transverse deficiency and for obtaining a space for alignment of the maxillary teeth in adult patients. Vinha et al.[10] insisted that increase in the oral cavity size could produce better positioning of the tongue, expand the nasal cavity and posterior pharyngeal space, and consequently reduce the airway obstruction in patients with OSAS.

Recently, Miniscrew-assisted RPE (MARPE) is introduced to correct the maxillary transverse discrepancy without surgical interventions in adults.[52.] Since miniscrews can help deliver the expansion force from RPE directly to the basal bone as a rigid element, MARPE without surgical interventions might have comparable effects with SARPE for non-growing patients.

5. Three-dimensional computational fluid dynamics

The CFD is defined as numerical methods and algorithms for analyzing the problems of fluid flow.[53] The 3D images are usually obtained from computed tomography (CT) or magnetic resonance images (MRI). The 3D-CFD can investigate functional imaging of the upper airway and analyze the flow characteristics through the upper airway.[54,55]

There are numerous 3D-CFD studies to investigate the OSAS in terms of the exploration of proper algorithms, validation of models, and diagnosis and treatment for clinical cases.[4,53,56-61]

6. Fluid structure interaction

The CFD models assume to have a rigid wall boundary and do not consider the interaction between flow and wall movement of the upper airway in OSAS

patients.[57,60,62,63] However, the FSI modeling can capture the biological flow features, motions, and deformations of the soft tissues. Therefore, it has gained an interest because of the potential impact in medical field.

However, there have been a limited number of FSI studies in OSAS research (particularly with experimental validation). There are only two tongue models[64,65] and one soft palate movement model.[66] Wang et al.[67] suggested that comparison of uvula displacement between pre- and post-surgical cases using FSI simulations could indicate the effect of nasal surgery on OSAS. Since these studies only modeled the upper airway structures partially such as the soft palate or tongue and assumed that the rest of the upper airway structures had a rigid wall[64,67] their upper airway FSI models were not experimentally validated.[23]

Considering the pharyngeal airway is not restricted by bony structures, lateral narrowing could be a dominant factor in collapse of the upper airway[68,69] Zhao et al.[23] insisted that the full pharyngeal FSI model could provide experimental validation and overcome the limitations of CFD. Zhao et al.[23] claimed that flow-induced pressure variations could be enough to induce the collapse of the pharynx. Since change in the air flow can prevent the collapse of air way, this phenomenon is important in treating OSAS.

III. Materials and Methods

Sample

A real OSAS patient (male, 18 years and 7 months old) was selected for the sample. He complained of crowding, protrusive lips, and uneasy breathing during sleep. Because he had a narrow maxillary basal arch and severe crowding, and refused to use an intraoral appliance or undergo MMA surgery, MARPE was selected as treatment method (Fig.1). He underwent in-laboratory polysomnography(PSG) at the T0 stage [body mass index (BMI), 25.0 kg/m^2; apnea and hypopnea index (AHI), 49.5 events/hour; respiratory disturbance index (RDI), 52.2 events/hour; lowest O_2 saturation rate (LSR), 85%]. After MARPE treatment at S-plant Dental Hospital, Seoul, Korea, his signs and symptoms of OSAS significantly resolved [age of 19 years and 1 month, BMI, 24.9 kg/m^2; AHI, 2.2 events/hour; RDI, 20.2 events/hour; LSR, 95%]. This study was reviewed and approved by the Institutional Review Board of School of Dentistry Seoul National University (S-D20170001).

Geometric Modeling

Cone beam computed tomograms (CBCT, iCAT, KAVO, Biberach, Germany; volume size: 23 cm in diameter X 17 cm in height, resolution: 0.3 voxel, exposure conditions: 37.1 mA and 120 kVp for 17.8 sec) were taken before (T0) and after MARPE therapy (T1, 6 months after T0). Although a standardized method for head and tongue posture during 3D image acquisitions is lacking, following instructions were given to the patient for the standardization in this study. The CBCTs were

taken his sitting at the natural head posture with the instruction of letter "N" tongue posture: place the tongue on the roof of the mouth directly behind the front teeth without pressing against the teeth and close the lips together.[70] The DICOM data of the T0 and T1 stages were exported to ICEM-CFD (ver. 15, ANSYS inc., Canonsburg, PA, USA) to fabricate the surface model (file type of STL). The 3D-computational models of the upper airway, including both the nasal cavity and the pharynx, were constructed. The meshes were generated with tetrahedron and prism elements. The total number of nodes and elements in each model is summarized in Table 1.

Computational FSI Simulation

FSI of the upper airway was performed under the following conditions: (1) The boundary condition at the nostril of an inlet was set to respiration cycle (5 seconds per cycle): 34.3 L/min (maximum inspiration), -2.5 L/min (resting), and -29.5 L/min (maximum expiration) (Fig. 3)[71]; (2) Material property: 7540 Pa of Young's modulus and 0.45 of Poisson's ratio[72] (3) In the nasal cavity area, 7 planes were set with an inter-plane distance of 10 mm from the aperture of the nostril to the posterior end of the nasal cavity (Fig. 2), and (4) In the pharynx area, 9 planes were set with an inter-plane distance of 10 mm from the beginning of the pharynx to the beginning of the larynx (Fig. 2). Respiratory cycle used in the simulation is enumerated in Fig. 3.

For the simulations of the airflow, the flow was assumed to be incompressible. The governing differential equations, the Reynolds-averaged Navier-Stokes equation for turbulence with the k - ε model, and constitutive equations for structure dynamics are shown in Table 2. Constant air density (1.185 kg/m^3) and viscosity (1.831×10^{-5} kg/m·s) were assumed. No-slip wall boundary conditions

were imposed on the airway walls.

The size of cross-sectional airway area and the pressure and velocity of airflow on each plane were analyzed at the T0 and T1 stages. Using the changes of each variable during T0-T1, the total resistance of airflow was calculated.

IV. Results

1. Changes in the cephalometric and model measurements (Tables 3 and 4)

The patient exhibited a Class II hyper-divergent skeletal pattern at the T0 stage (ANB, 8.9°; FMA, 50.3°; Table 3). The values of cephalometric measurements were not significantly changed at the T1 stage (ANB, 8.4°; FMA, 50.8°; Table 3). However, after MARPE therapy, the maxillary dental arch was significantly enlarged with a decreasing order from inter-first premolar width, inter-second premolar width, to inter-first molar width measured from study models at T0 and T1 (7.2 mm, 6.1 mm, and 4.9 mm, respectively, Table 4).

2. Changes in the cross-sectional airway area (Table 5)

In the nasal cavity, there was a significant increase at the planes 1 to 3 (0.86 cm^2 to 1.16 cm^2, 38.5% to 53.3%), and a moderate increase at the planes 4 to 6 (0.65 cm^2 to 1.04 cm^2, 27.5% to 38.8%). However, the plane 7 showed only a slight increase. In the pharynx, the planes 1 to 4 showed a strong increasing trend (1.39 cm^2 to 1.69 cm^2, 40.4% to 67.3%), which weakened at the plane 5 and then disappeared at the planes 6 to 9. These findings imply that the effect of MARPE mainly existed at the anterior and middle parts of the nasal cavity and propagated to the nasopharynx (planes 1 and 2) and the upper and middle part of the oropharynx (planes 3,4, and 5). When the amounts of increase in the cross-sectional airway area were compared, the values of the pharynx were larger than

those of the nasal cavity although the pharynx was located farther from the nasal cavity where MARPE was placed.

3. Changes in the pressure and velocity of airflow (Tables 6 and 7, Figs. 4 and 5)

At the planes 1 to 7 in the nasal cavity and at the planes 1 to 5 in the pharynx, the absolute values of pressure and velocity at maximum inspiration, rest, and maximum expiration after MARPE were lower than those before MARPE.

In the nasal cavity, at the maximum inspiration, there was a significant decrease in the pressure values at the planes 1 to 4 (-29.3 Pa to -10.2 Pa, -52.9% to -33.3%) and in the velocity values at the planes 1, 2, 3, and 7 (range: -0.98 m/s to -1.44 m/s; -29.9% to -37.9%). At the rest, there was a slight decrease in the pressure and no significant change in the velocity at all seven planes. At the maximum expiration, there was a decrease in the pressure from the planes 1 to 7 (26.2 Pa to 2.8 Pa, -53.6% to -17.5%) and a decrease in the velocity at the planes 1 to 3 (-0.87 m/s to -1.54 m/s; -35.9% to -42.6%).

In the pharynx, at the maximum inspiration, there was a considerable decrease in the pressure at the planes 1 to 7 (-9.6 Pa to -10.8 Pa and -34.1% to -37.0%) and a significant decrease at the planes 8 and 9 (-12.6 Pa, -66.9%; -13.5 Pa, -67.5%, respectively). There was also a significant decrease in the velocity at the planes 1 to 4 (-0.61 m/s to -1.01 m/s and -31.1% to -41.3%), a moderate decrease at the planes 5 to 7, and no significant change at the planes 8 and 9. However, at the rest, there were no significant changes in pressure and velocity at any of the nine planes. At the maximum expiration, there was a steady pressure drop at the planes 1 to 7 and a substantial drop at the planes 8 (9.4 Pa, -73.9%) and 9 (8.9 Pa, -68.9%). There was also a decrease in the velocity at the planes 1 through 5.

4. Changes in the node displacement of the airway wall (Table 8 and Fig. 6)

In both the nasal cavity and the pharynx, there was a pattern of decrease in the node displacement value from maximum inspiration to rest and a pattern of increase from rest to maximum expiration over the entire areas, especially after MARPE. However, there was no clinically meaningful change in the absolute values, regardless of respiration stage. These findings indicate that changes in the pressure and velocity of airflow (Tables 6 and 7) did not affect the node displacement of the airway wall in both the nasal cavity and the pharynx (Table 8).

5. Changes in average pressure, flow rate, and total resistance (Table 9)

Since there was a significant decrease in the average pressure at the maximum inspiration (-55.5%), rest (-49.7%), and maximum expiration (-52.6%) during T0-T1, the total resistance was significantly decreased at the maximum inspiration (-55.1%), rest (-35.9%), and maximum expiration (-33.9%).

V. DISCUSSION

1. Changes in the cross-sectional airway area

The amounts of increase in the cross-sectional airway area after MARPE were significantly larger at the anterior part than the posterior part in the nasal cavity (Table 5), and this propagated down to the nasopharynx (planes 1 and 2) and the upper and middle part of oropharynx (planes 3, 4, and 5) (Table 5). Due to anatomical continuity of the nasal cavity and the pharynx, transverse expansion of the hard palate by MARPE could directly increase the size of cross-sectional airway area at the nasal cavity and indirectly at the pharynx. These results are in agreement with previous studies, which showed enlargement of the pharyngeal airway in children by conventional RPE [73] and in adults by SARPE.[10]

The reason that the amounts of increase in the cross-sectional area of the nasal cavity was smaller than the pharynx (Table 5) is considered as the nasal cavity is a complex structure mainly composed of the hard tissues such as the nasal septum, conchae, and palatal bone, while the pharynx is a relatively simple tubing system made of the soft tissue.

2. Changes in the pressure and velocity of airflow

A pressure drop existed in the entire nasal cavity and the pharynx at the maximum inspiration and the maximum expiration. Decrease in airflow velocity existed primarily in the anterior part of the nasal cavity at both maximum inspiration and maximum expiration and propagated into the nasopharynx (planes 1 and 2) and the upper and middle part of oropharynx (planes 3, 4, and 5) at the

maximum inspiration (Tables 6 and 7, Figs. 4 and 5). Although the nasal cavity exhibited smaller amounts of increase in the cross-sectional airway area compared to the pharynx (Table 5), the nasal cavity had greater amounts of decrease in both pressure and velocity compared to the pharynx. The reason seems that the anterior part of the nasal cavity plays an important role as the main entrance and exit for airflow and reduces the airflow resistance in the upper airway (Tables 6 and 7). The impact of nasal cavity expansion might reach down to the middle part of the oropharynx (Tables 6 and 7, Figs. 4 and 5). These results are in accordance with Iwasaki et al[28] However, as their study modeled only the nasal cavity,[28] there are some limitations to generalize their data when considered the whole process of respiration.

As the amounts of difference in the pressure and velocity between inspiration and expiration were diminished, respectively (Tables 6 and 7, Figs. 4 and 5), it can be stated that the gradient of airflow became smoother and the quality of respiration improved.

3. Changes in the node displacement of the airway wall

In the present study, the amounts of node displacement in both the nasal cavity and the pharynx were too small to be considered clinically meaningful (Table 8 and Fig. 6), which was not concordant with previous FSI study by Zhao et al[23]. They reported that the amounts of node displacement in the pharynx appeared to be significant.[23] However, their study had some limitations because the nasal cavity was not included in 3D computational modeling.[23] Therefore, the findings from this study suggested that the airway wall in the nasal cavity and the pharynx would not move during the respiratory cycle as much as reported by Zhao et al.[23] In other words, the amounts of node displacement in the pharynx turned into insignificant when the nasal cavity was included in FSI analysis.

4. Changes in the average pressure, flow rate, and total resistance

In this study, MARPE significantly reduced total resistance in the upper airway during the entire respiratory cycle (Table 9). This is in accordance with the conclusion from a previous review article of Neeley et al,[74] which suggested that expansion of the nasal cavity floor can give benefits to patients who have a constricted maxillary arch and a nasal airflow problem.

Since this study included the nasal cavity in a 3D computational model and used the FSI analysis, our results may reveal more realistic effects of MARPE on changes in airflow of OSAS patients compared to previous studies.[10, 23, 28, 73] However, further studies will be needed to use CT data of OSA patients taken in the supine position and to find more realistic values of material properties of the upper airway for better CFD/FSI model. And it should also be endeavored to investigate other treatment modalities for OSAS (e.g. intraoral appliance, soft tissue procedures, and MMA) with a large sample size.

The originality of this study can be considered as follows:

1) Inclusion of the nasal cavity in CFD/FSI analysis
2) Investigation of the effectiveness of MARPE on adult OSAS treatment
3) Realistic approach for respiration cycle (5 seconds per cycle)

However, a cautious interpretation of the results is recommended for a real clinical situation of OSAS.

VI. CONCLUSION

3D-CFD/FSI analysis with appropriate model incorporating the nasal cavity and pharynx showed improvement of airflow and reduction of resistance in the upper airway after MARPE therapy. Since MARPE improved airflow and reduced resistance in the upper airway of 3D computational models, there is high possibility for MARPE to be an alternative treatment modality for adult patients with who have moderate to severe narrow basal arch and crowding and refuse to the intraoral appliance or MMA surgery.

Reference

1. Ahn HW, Cho IS, Cho KC, Choi JY, Chung JW, Baek SH. Surgical treatment modality for facial esthetics in an obstructive sleep apnea patient with protrusive upper lip and acute nasolabial angle. Angle Orthod 2013;83:355–63.

2. Phillips B, Cook Y, Schmitt F, Berry D. Sleep apnea: prevalence of risk factors in a general population. South Med J. 1989;82:1090-2.

3. Epstein LJ, Kristo D, Strollo PJ, Friedman N, Malhotra A, Patil SP, et al. Clinical guideline for the evaluation, management and long-term care of obstructive sleep apnea in adults. J Clin Sleep Med 2009;5:263–76.

4. Kim T, Kim HH, Hong SO, Baek SH, Kim KW, Suh SH, et al. Change in the Upper Airway of Patients With Obstructive Sleep Apnea Syndrome Using Computational Fluid Dynamics Analysis: Conventional Maxillomandibular Advancement Versus Modified Maxillomandibular Advancement With Anterior Segmental Setback Osteotomy. J Craniofac Surg 2015;26:e765–70.

5. Katyal V, Pamula Y, Daynes CN, Martin J, Dreyer CW, Kennedy D, et al. Craniofacial and upper airway morphology in pediatric sleep-disordered breathing and changes in quality of life with rapid maxillary expansion. Am J Orthod Dentofacial Orthop 2013;144:860–71.

6. Villa MP, Rizzoli A, Rabasco J, Vitelli O, Pietropaoli N, Cecili M et al. Rapid maxillary expansion outcomes in treatment of obstructive sleep apnea in children. Sleep Med 2015;16:709–16.

7. Taddei M, Alkhamis N, Tagariello T, D'Alessandro G, Mariucci EM, Piana G. Effects of rapid maxillary expansion and mandibular advancement on upper

airways in Marfan's syndrome children: a home sleep study and cephalometric evaluation. Sleep Breath 2015;19:1213–20.

8. Pereira-Filho VA, Monnazzi MS, Gabrielli MAC, Spin-Neto R, Watanabe ER, Gimenez CMM, et al. Volumetric upper airway assessment in patients with transverse maxillary deficiency after surgically assisted rapid maxillary expansion. Int J Oral Maxillofac Surg 2014;43:581–6.

9. Jaipal PR, Rachala MR, Rajan R, Jhawar DK, Ankush B. Management of Adult Transverse Malocclusion with Surgically Assisted Rapid Palatal Expansion. J Clin Diagn Res 2016;10:ZJ10–2.

10. Vinha PP, Faria AC, Xavier SP, Christino M, de Mello-Filho FV. Enlargement of the Pharynx Resulting From Surgically Assisted Rapid Maxillary Expansion. J Oral Maxillofac Surg 2016;74:369–79.

11. Wilmes B, Nienkemper M, Drescher D. Application and effectiveness of a mini-implant-and tooth-borne rapid palatal expansion device: the hybrid hyrax. World J Orthod 2010;11:323–330.

12. Choi SH, Shi KK, Cha JY, Park YC, Lee KJ. Nonsurgical miniscrew-assisted rapid maxillary expansion results in acceptable stability in young adults. Angle Orthod 2016;86:713–20.

13. Suzuki H, Moon W, Previdente LH, Suzuki SS, Garcez AS, Consolaro A. Miniscrew-assisted rapid palatal expander (MARPE): the quest for pure orthopedic movement. Dental Press J Orthod 2016;21:17–23.

14. Kabalan O, Gordon J, Heo G, Lagravère MO. Nasal airway changes in bone-borne and tooth-borne rapid maxillary expansion treatments. Int Orthod 2015;13:1–15.

15. Battagel JM, L'Estrange PR, Nolan P, Harkness B. The role of lateral cephalometric radiography and fluoroscopy in assessing mandibular advancement in sleep-related disorders. Eur J Orthod. 1998;20:121-32.

16. Isono S, Morrison DL, Launois SH, Feroah TR, Whitelaw WA, Remmers JE. Static mechanics of the velopharynx of patients with obstructive sleep apnea. J Appl Physiol (1985). 1993;75:148-54.

17. Li HY, Chen NH, Wang CR, Shu YH, Wang PC. Use of 3-dimensional computed tomography scan to evaluate upper airway patency for patients undergoing sleep-disordered breathing surgery. Otolaryngol Head Neck Surg. 2003;129:336-42.

18. Schendel S, Powell N, Jacobson R. Maxillary, mandibular, and chin advancement: treatment planning based on airway anatomy in obstructive sleep apnea. J Oral Maxillofac Surg. 2011;69:663-76.

19. Abramson Z, Susarla SM, Lawler M, Bouchard C, Troulis M, Kaban LB. Three-dimensional computed tomographic airway analysis of patients with obstructive sleep apnea treated by maxillomandibular advancement. J Oral Maxillofac Surg. 2011;69:677-86.

20. Abramson Z, Susarla S, August M, Troulis M, Kaban L. Three-dimensional computed tomographic analysis of airway anatomy in patients with obstructive sleep apnea. J Oral Maxillofac Surg. 2010;68:354-62.

21. Guijarro-Martínez R, Swennen GR.Cone-beam computerized tomography imaging and analysis of the upper airway: a systematic review of the literature. Int J Oral Maxillofac Surg. 2011;40:1227-37.

22. Mylavarapu G1, Mihaescu M, Fuchs L, Papatziamos G, Gutmark E. Planning human upper airway surgery using computational fluid dynamics. J Biomech. 2013;46:1979-86.

23. Zhao M, Barber T, Cistulli PA, Sutherland K, Rosengarten G: Simulation of upper airway occlusion without and with mandibular advancement in obstructive sleep apnea using fluid-structure interaction. J Biomech. 2013;46:2586-92.

24. Pirnar J, Dolenc-Grošelj L, Fajdiga I, Žun I. Computational fluid-structure interaction simulation of airflow in the human upper airway. J Biomech 2015;48:3685–91.

25. Shah DH, Kim KB, McQuilling MW, Movahed R, Shah AH, Kim YI. Computational fluid dynamics for the assessment of upper airway changes in skeletal Class III patients treated with mandibular setback surgery. Angle Orthod 2016;86:976–82.

26. Liu SYC, Huon LK, Iwasaki T, Yoon A, Riley R, Powell N, et al. Efficacy of Maxillomandibular Advancement Examined with Drug-Induced Sleep Endoscopy and Computational Fluid Dynamics Airflow Modeling. Otolaryngol Head Neck Surg 2016;154:189–95.

27. Cheng GC, Koomullil RP, Ito Y, Shih AM, Sittitavornwong S, Waite PD. Assessment of Surgical Effects on Patients with Obstructive Sleep Apnea Syndrome Using Computational Fluid Dynamics Simulations. Math Comput Simul 2014;106:44–59.

28. Iwasaki T, Saitoh I, Takemoto Y, Inada E, Kanomi R, Hayasaki H, et al. Improvement of nasal airway ventilation after rapid maxillary expansion evaluated

with computational fluid dynamics. Am J Orthod Dentofacial Orthop 2012;141:269–78.

29. Cisonni J, Lucey AD, King AJC, Islam SMS, Lewis R, Goonewardene MS. Numerical simulation of pharyngeal airflow applied to obstructive sleep apnea: effect of the nasal cavity in anatomically accurate airway models. Med Biol Eng Comput 2015;53:1129–39.

30. Guilleminault C, Tilkian A, Dement WC: The Sleep Apnea Syndromes. Annu Rev Med. 1976;27:465-84.

31. Kripke DF, Ancoli-Israel S, Klauber MR, Wingard DL, Mason WJ, Mullaney DJ. Prevalence of sleep-disordered breathing in ages 40-64 years: a population-based survey. Sleep. 1997;20:65-76.

32. Young T, Palta M, Dempsey J, Skatrud J, Weber S, Badr S. The Occurrence of Sleep-Disordered Breathing among Middle-Aged Adults. N Engl J Med. 1993;328:1230-5.

33. Malhotra A, White DP. Obstructive sleep apnoea. Lancet. 2002;360:237-45.

34. Younes M. Contributions of Upper Airway Mechanics and Control Mechanisms to Severity of Obstructive Apnea. Am J Respir Crit Care Med. 2003;168:645-58.

35. Schwab RJ, Pasirstein M, Pierson R, Mackley A, Hachadoorian R, Arens R, Maislin G, Pack AI. Identification of Upper Airway Anatomic Risk Factors for Obstructive Sleep Apnea with Volumetric Magnetic Resonance Imaging. Am J Respir Crit Care Med. 2003;168:522-30.

36. Fogel RB, Malhotra A, White DP: Sleep. 2: pathophysiology of obstructive sleep apnoea/hypopnoea syndrome. Thorax. 2004;59:159-63.

37. Leiter JC. Upper airway shape: Is it important in the pathogenesis of obstructive sleep apnea? Am J Respir Crit Care Med. 1996;153:894-8.

38. Giles TL, Lasserson TJ, Smith B, White J, Wright JJ, Cates CJ. Continuous Positive Airways Pressure for Obstructive Sleep Apnoea in Adults. Cochrane Database Syst Rev. 2006;19:1-113

39. Engleman HM, Wild MR. Improving CPAP use by patients with the sleep apnoea/hypopnoea syndrome (SAHS). Sleep Med Rev. 2003;7:81-99.

40. Reishtein JL, Maislin G, Weaver TE, Multisite Study group. Outcome of CPAP treatment on intimate and sexual relationships in men with obstructive sleep apnea. J Clin Sleep Med. 2010;6:221-6.

41. Schmidt-Nowara W, Lowe A, Wiegand L, Cartwright R, Perez-Guerra F, Menn S. Oral appliances for the treatment of snoring and obstructive sleep apnea: a review. Sleep. 1995;18:501-10.

42. Richard W, Kox D, Herder den C, van Tinteren H, de Vries N. One stage multilevel surgery (uvulopalatopharyngoplasty, hyoid suspension, radiofrequent ablation of the tongue base with/without genioglossus advancement), in obstructive sleep apnea syndrome. Eur Arch Otorhinolaryngol. 2007;264:439-44.

43. Sher AE, Schechtman KB, Piccirillo JF. The efficacy of surgical modifications of the upper airway in adults with obstructive sleep apnea syndrome. Sleep. 1996;19:156-77.

44. Holty JE, Guilleminault C. Maxillomandibular advancement for the treatment of obstructive sleep apnea: a systematic review and meta-analysis. Sleep Med Rev. 2010;14:287-97.

45. Tsui WK, Yang Y, Cheung LK, Leung YY. Distraction osteogenesis as a treatment of obstructive sleep apnea syndrome: A systematic review. Medicine (Baltimore). 2016;95:e4674.

46. Pirelli P, Saponara M, De Rosa C, Fanucci E. Orthodontics and Obstructive Sleep Apnea in Children. Med Clin North Am. 2010;94:517-29.

47. Camacho M, Chang ET, Song SA, Abdullatif J, Zaghi S, Pirelli P, Certal V, Guilleminault C. Rapid maxillary expansion for pediatric obstructive sleep apnea: A systematic review and meta-analysis. Laryngoscope. 2016;00:1-8

48. Huynh NT, Desplats E, Almeida FR. Orthodontics treatments for managing obstructive sleep apnea syndrome in children: A systematic review and meta-analysis. Sleep Med Rev. 2016;25:84-94.

49. Vidya VS, A. Sumathi F. Rapid Maxillary Expansion as a Standard Treatment for Obstructive Sleep Apnea Syndrome: A Systematic Review. IOSR Journal of Dental and Medical Sciences 2015;1:51–5.

50. Vinha PP, Eckeli AL, Faria AC, Xavier SP, de Mello-Filho FV. Effects of surgically assisted rapid maxillary expansion on obstructive sleep apnea and daytime sleepiness. Sleep Breath. 2016;20:501-8.

51. Koudstaal MJ, Poort LJ, van der Wal KGH, Wolvius EB, Prahl-Andersen B, Schulten AJM. Surgically assisted rapid maxillary expansion (SARME): a review of the literature. Int J Oral Maxillofac Surg. 2005;34:709-14.

52. Moon W, Wu KW, MacGinnis M, Sung J, Chu H, Youssef G, Machado A. The efficacy of maxillary protraction protocols with the micro-implant-assisted rapid palatal expander (MARPE) and the novel N2 mini-implant—a finite element study. Prog Orthod. 2015;16:1-14.

53. Yu CC, Hsiao HD, Tseng TI, Lee LC, Yao CM, Chen NH, Wang CJ, Chen YR. Computational fluid dynamics study of the inspiratory upper airway and clinical severity of obstructive sleep apnea. J Craniofac Surg. 2012;23:401-5.

54. Yang XL, Liu Y, Luo HY. Respiratory flow in obstructed airways. J Biomech. 2006;39:2743-51.

55. Luo XY, Hinton JS, Liew TT, Tan KK. LES modelling of flow in a simple airway model. Med Eng Phys. 2004;26:403-13.

56. Sung SJ, Jeong SJ, Yu YS, Hwang CJ, Pae EK. Customized three-dimensional computational fluid dynamics simulation of the upper airway of obstructive sleep apnea. Angle Orthod. 2006;76:791-9.

57. Xu C, Sin S, McDonough JM, Udupa JK, Guez A, Arens R, Wootton DM. Computational fluid dynamics modeling of the upper airway of children with obstructive sleep apnea syndrome in steady flow. J Biomech. 2006;39:2043-54.

58. Mihaescu M, Murugappan S, Gutmark E, Donnelly LF, Kalra M. Computational Modeling of Upper Airway Before and After Adenotonsillectomy for Obstructive Sleep Apnea. Laryngoscope. 2008;118:360-2.

59. Mylavarapu G, Murugappan S, Mihaescu M, Kalra M, Khosla S, Gutmark E. Validation of computational fluid dynamics methodology used for human upper airway flow simulations. J Biomech. 2009;42:1553-9.

60. Jeong SJ, Kim WS, Sung SJ. Numerical investigation on the flow characteristics and aerodynamic force of the upper airway of patient with obstructive sleep apnea using computational fluid dynamics. Med Eng Phys. 2007;29:637-51.

61. Vos W, De Backer J, Devolder A, Vanderveken O, Verhulst S, Salgado R, Germonpre P, Partoens B, Wuyts F, Parizel P, De Backer W. Correlation between severity of sleep apnea and upper airway morphology based on advanced anatomical and functional imaging. J Biomech. 2007;40:2207-13.

62. Wang Y, Liu Y, Sun X, Yu S, Gao F. Numerical analysis of respiratory flow patterns within human upper airway. Acta Mech Sin. 2009;25:737–46.

63. Van Holsbeke C, De Backer J, Vos W, Verdonck P, Van Ransbeeck P, Claessens T, Braem M, Vanderveken O, De Backer W. Anatomical and functional changes in the upper airways of sleep apnea patients due to mandibular repositioning: A large scale study. J Biomech. 2011;44:442-9.

64. Chouly F, Van Hirtum A, Lagrée PY, Pelorson X, Payan Y. Numerical and experimental study of expiratory flow in the case of major upper airway obstructions with fluid–structure interaction. Journal of Fluids and Structures 2008;24:250–69.

65. Rasani MR, Inthavong K, Tu JY. Simulation of pharyngeal airway interaction with air flow using low-re turbulence model. Modelling and Simulation in Engineering 2011;2011:5–9.

66. Sun X, Yu C, Wang Y, Liu Y. Numerical simulation of soft palate movement and airflow in human upper airway by fluid-structure interaction method. Acta Mech Sin 2007;23:359–67.

67. Wang Y, Wang J, Liu Y, Yu S, Sun X, Li S, Shen S, Zhao W. Fluid-structure interaction modeling of upper airways before and after nasal surgery for obstructive sleep apnea. Int J Numer Method Biomed Eng 2012;28:528–46.

68. Ayappa I, Rapoport DM. The upper airway in sleep: physiology of the pharynx. Sleep Med Rev. 2003;7:9-33.

69. Pohunek P. Development, structure and function of the upper airways. Paediatr Respir Rev. 2004;5:2-8.

70. Gurani SF, Di Carlo G, Cattaneo PM, Thorn JJ, Pinholt EM. Effect of Head and Tongue Posture on the Pharyngeal Airway Dimensions and Morphology in Three-Dimensional Imaging: a Systematic Review. J Oral Maxillofac Res. 2016;7:e1.

71. Scurr C, Feldman SA, Soni N. Scientific Foundations of Anaesthesia. Oxford:Butterworth-Heinemann 1990; 235–42.

72. Cheng S, Gandevia SC, Green M, Sinkus R, Bilston LE. Viscoelastic properties of the tongue and soft palate using MR elastography. J Biomech. 2011;44:450-4.

73. Iwasaki T, Saitoh I, Takemoto Y, Inada E, Kakuno E, Kanomi R, Hayasaki H, Yamasaki Y. Tongue posture improvement and pharyngeal airway enlargement as secondary effects of rapid maxillary expansion: a cone-beam computed tomography study. Am J Orthod Dentofacial Orthop. 2013;143:235-45.

74. Neeley WW II, Edgin WA, Gonzales DA. A Review of the Effects of Expansion of the Nasal Base on Nasal Airflow and Resistance. J Oral Maxillofac Surg. 2007;65:1174-9.

Table 1. Numbers of the nodes and elements before (T0) and after miniscrew-assisted rapid palatal expansion (MARPE, T1)

Number	T0		T1	
	nodes	elements	nodes	elements
CFD	56558	251893	59495	265830
FSI	1522662	6659746	139251	723473

CFD, computational fluid dynamics; FSI, fluid-structure interaction.

Table 2. The governing equations for numerical turbulence model

Category	**Equation**
Differential equation	$\frac{\partial u_i}{\partial x_i} = 0$ $\rho\frac{\partial u_i}{\partial t} + u_j\frac{\partial u_i}{\partial x_j} = -\frac{\partial p}{\partial x_i} + \frac{\partial}{\partial x_j}[\mu_{eff}(\frac{\partial u_i}{\partial x_j} + \frac{\partial u_j}{\partial x_i}) - \rho\overline{u}_i'\overline{u}_j']$
the Reynolds-averaged Navier-Stokes equation with the k –ε model	$\mu_{eff} = \mu + \mu_t$, $\mu_t = C_\mu\rho\frac{k^2}{\varepsilon}$ $\frac{\partial(\rho k)}{\partial t} + \frac{\partial(\rho k u_j)}{\partial x_j} = \frac{\partial}{\partial x_j}[(\mu + \frac{\mu_t}{\sigma_k})\frac{\partial k}{\partial x_j}] + P_k - \rho\varepsilon + P_{kb}$ $\frac{\partial(\rho\varepsilon)}{\partial t} + \frac{\partial(\rho\varepsilon u_j)}{\partial x_j} = \frac{\partial}{\partial x_j}[(\mu + \frac{\mu_t}{\sigma_\varepsilon})\frac{\partial\varepsilon}{\partial x_j}] + \frac{\varepsilon}{k}(C_{\varepsilon1}P_k - C_{\varepsilon2}\rho\varepsilon + C_{\varepsilon1}P_{\varepsilon b})$
Constitutive equation	$\rho a_i = \sigma_{ij,j} + \rho f_i$, $\sigma_{ij} = D_{ijkl}\varepsilon_{kl}$ $a_i = \frac{d\hat{u}_i}{dt}$, $\sigma_{ij}n_i = T_i$

* where t is the time on the structure domain, n_i is the unit outward pointing normal on the wall surface, T_i is the surface traction vector at time t, σ_{ij} is the mechanical stress tensor, D_{ijkl} is the Lagrangian elasticity tensor, and ε_{kl} is the strain tensor.

Table 3. Comparison of the cephalometric measurements at the T0 and T1 stages

Variables	Norm*	T0	T1
SNA (°)	81.28	76.28	76.90
SNB (°)	78.91	67.42	68.51
ANB (°)	2.69	8.86	8.39
A-N perp.(mm)	-0.79	-6.24	-6.77
Pog-N perp.(mm)	-2.26	-31.38	-31.66
FMA (°)	26.21	50.28	50.84
U1-SN (°)	107.01	87.45	91.83
IMPA (°)	95.85	75.54	80.28

Norm values are from Sung et al (2001).[22]5

Variables *	T0	T1	ΔT1-T0
Inter-first premolar width (mm)	35.34	42.52	7.18
Inter-second premolar width (mm)	44.15	50.36	6.12
Inter-first molar width (mm)	51.67	56.58	4.91
Arch length discrepancy (mm)	-15.67	-12.86	2.81

Table 4. Comparison of the maxillary dental arch width at the T0 and T1 stages

*Due to ectopic eruption of the maxillary canines, inter-canine width was not included in this table.

Table 5. Changes in the cross-sectional airway area during T0-T1 stages

	Airway area [cm^2]	Before MARPE (T0)	After MARPE (T1)	ΔT1-T0	Percentage of change [(ΔT1-T0)/T0]x100
Nasal cavity	Plane 1	2.49	3.44	0.96	38.51
	Plane 2	1.63	2.48	0.86	52.62
	Plane 3	2.17	3.33	1.16	53.27
	Plane 4	2.33	2.98	0.65	27.98
	Plane 5	2.57	3.27	0.71	27.51
	Plane 6	2.69	3.73	1.04	38.78
	Plane 7	5.54	6.13	0.58	10.54
Pharynx	Plane 1	3.43	4.82	1.39	40.42
	Plane 2	2.95	4.64	1.69	57.41
	Plane 3	2.51	4.20	1.69	67.28
	Plane 4	2.80	4.48	1.69	60.22
	Plane 5	3.24	4.28	1.04	31.92
	Plane 6	3.73	4.10	0.36	9.70
	Plane 7	4.77	4.75	-0.02	-0.32
	Plane 8	4.36	4.54	0.18	4.10
	Plane 9	3.72	3.75	0.03	0.89

Table 6. Changes in the pressure of airflow during T0-T1 stages

Pressure (Pa)		Before MARPE (T0)			After MARPE (T1)			ΔT1-T0			Percentage of change [(ΔT1-T0)/T0]x100		
		Max. Inspiration	Rest	Max. Expiration	Max. Inspiration	Rest	Max. Expiration	Max. Inspiration	Rest	Max. Expiration	Max. Inspiration	Rest	Max. Expiration
		1.080 s	1.730 s	2.805 s	1.080 s	1.730 s	2.805 s	1.080 s	1.730 s	2.805 s	1.080 s	1.730 s	2.805 s
Nasal cavity	Plane 1	55.45	-6.77	-48.81	26.13	-3.46	-22.65	-29.32	3.31	26.16	-52.88	-48.87	-53.60
	Plane 2	45.82	-6.07	-45.17	24.62	-3.21	-21.47	-21.20	2.86	23.70	-46.27	-47.06	-52.47
	Plane 3	35.92	-4.56	-32.98	21.75	-2.76	-19.15	-14.17	1.81	13.83	-39.45	-39.58	-41.94
	Plane 4	30.54	-3.50	-24.96	20.38	-2.42	-17.51	-10.16	1.07	7.45	-33.27	-30.69	-29.85
	Plane 5	29.58	-2.75	-20.51	19.98	-1.99	-15.44	-9.60	0.76	5.07	-32.45	-27.52	-24.72
	Plane 6	29.33	-2.24	-17.78	19.29	-1.69	-13.93	-10.04	0.55	3.85	-34.23	-24.68	-21.65
	Plane 7	28.78	-1.98	-16.05	18.56	-1.54	-13.25	-10.22	0.45	2.80	-35.51	-22.58	-17.45
Pharynx	Plane 1	29.28	-1.90	-16.05	18.45	-1.44	-13.25	-10.83	0.46	2.80	-36.99	-24.17	-17.45
	Plane 2	29.01	-1.85	-16.51	18.54	-1.38	-13.20	-10.47	0.47	3.31	-36.09	-25.53	-20.05
	Plane 3	27.97	-1.75	-16.78	18.42	-1.33	-13.19	-9.55	0.42	3.59	-34.14	-24.14	-21.40
	Plane 4	28.03	-1.62	-16.77	18.42	-1.27	-13.10	-9.61	0.35	3.67	-34.29	-21.42	-21.88
	Plane 5	28.42	-1.52	-16.81	18.34	-1.24	-13.49	-10.08	0.29	3.32	-35.47	-18.84	-19.75
	Plane 6	28.76	-1.51	-17.18	18.20	-1.26	-13.89	-10.56	0.25	3.29	-36.72	-16.80	-19.15
	Plane 7	25.38	-1.40	-15.39	14.64	-1.15	-12.10	-10.74	0.25	3.29	-42.32	-17.68	-21.38
	Plane 8	18.86	-0.81	-12.72	6.25	-0.40	-3.33	-12.61	0.41	9.39	-66.86	-50.33	-73.85
	Plane 9	19.99	-0.98	-12.84	6.51	-0.42	-4.00	-13.49	0.56	8.85	-67.46	-57.12	-68.89

Table 7. Changes in the velocity of airflow during T0-T1 stages

Velocity [m/s]		Before MARPE (T0)			After MARPE (T1)			ΔT1-T0			percentage of change [(ΔT1-T0)/T0]x100		
		Max. Inspiration	Rest	Max. Expiration	Max. Inspiration	Rest	Max. Expiration	Max. Inspiration	Rest	Max. Expiration	Max. Inspiration	Rest	Max. Expiration
		1.080 s	1.730 s	2.805 s	1.080 s	1.730 s	2.805 s	1.080 s	1.730 s	2.805 s	1.080 s	1.730 s	2.805 s
Nasal cavity	Plane 1	3.28	0.70	3.22	2.30	0.49	1.85	-0.98	-0.21	-1.37	-29.93	-30.29	-42.64
	Plane 2	3.89	0.86	3.65	2.45	0.54	2.11	-1.44	-0.33	-1.54	-37.0	-37.82	-42.25
	Plane 3	2.90	0.63	2.42	1.80	0.41	1.56	-1.10	-0.22	-0.87	-37.93	-35.38	-35.85
	Plane 4	2.61	0.58	2.22	1.98	0.45	1.70	-0.63	-0.14	-0.52	-23.98	-23.10	-23.31
	Plane 5	2.40	0.53	2.04	1.83	0.43	1.60	-0.56	-0.11	-0.44	-23.53	-20.57	-21.64
	Plane 6	2.76	0.55	2.07	1.77	0.40	1.54	-0.99	-0.15	-0.54	-35.71	-27.05	-25.95
	Plane 7	2.06	0.35	1.29	1.47	0.31	1.25	-0.58	-0.05	-0.05	-28.34	-12.79	-3.49
Pharynx	Plane 1	1.96	0.40	1.62	1.35	0.32	1.24	-0.61	-0.09	-0.38	-31.14	-21.83	-23.57
	Plane 2	2.20	0.47	1.90	1.35	0.30	1.31	-0.85	-0.16	-0.59	-38.64	-34.91	-31.13
	Plane 3	2.45	0.53	2.14	1.44	0.32	1.52	-1.01	-0.21	-0.62	-41.30	-39.15	-28.93
	Plane 4	2.16	0.48	1.98	1.33	0.31	1.56	-0.83	-0.17	-0.42	-38.27	-35.30	-21.34
	Plane 5	1.84	0.41	1.79	1.38	0.33	1.66	-0.46	-0.08	-0.12	-25.14	-20.16	-6.83
	Plane 6	1.63	0.40	1.69	1.46	0.39	1.86	-0.17	-0.01	0.17	-10.55	-2.24	9.76
	Plane 7	2.30	0.39	1.96	2.02	0.40	2.19	-0.28	0.01	0.23	-12.14	3.60	11.77
	Plane 8	2.07	0.42	2.18	2.07	0.38	1.64	-0.01	-0.03	-0.54	-0.29	-7.69	-24.67
	Plane 9	2.88	0.44	1.94	3.02	0.39	1.59	0.14	-0.06	-0.35	4.68	-12.94	-17.93

Table 8. Changes in the displacement of nodes in the soft tissue of the airway wall during T0-T1 stages

Displacement [mm]		Before MARPE (T0)			After MARPE (T1)			ΔT1-T0		
		Max. Inspiration	Rest	Max. Expiration	Max. Inspiration	Rest	Max. Expiration	Max. Inspiration	Rest	Max. Expiration
		1.080 s	1.730 s	2.805 s	1.080 s	1.730 s	2.805 s	1.080 s	1.730 s	2.805 s
Nasal cavity	Plane 1	1.48E-10	2.52E-11	1.24E-10	4.03E-10	8.89E-11	3.72E-10	2.55E-10	6.37E-11	2.48E-10
	Plane 2	2.09E-10	4.13E-11	1.98E-10	6.82E-10	1.82E-10	6.56E-10	4.73E-10	1.41E-10	4.58E-10
	Plane 3	2.55E-10	5.28E-11	2.38E-10	9.04E-10	2.36E-10	8.63E-10	6.49E-10	1.83E-10	6.25E-10
	Plane 4	2.51E-10	5.86E-11	2.23E-10	9.66E-10	2.76E-10	9.09E-10	7.15E-10	2.17E-10	6.86E-10
	Plane 5	2.11E-10	6.03E-11	1.65E-10	8.20E-10	2.77E-10	7.17E-10	6.09E-10	2.17E-10	5.52E-10
	Plane 6	1.81E-10	6.38E-11	1.24E-10	6.46E-10	2.67E-10	4.73E-10	4.65E-10	2.03E-10	3.49E-10
	Plane 7	1.61E-10	5.85E-11	7.25E-11	6.06E-10	2.25E-10	3.08E-10	4.45E-10	1.67E-10	2.36E-10
Pharynx	Plane 1	3.03E-07	5.91E-08	1.35E-07	1.42E-06	3.11E-07	8.62E-07	1.12E-06	2.52E-07	7.27E-07
	Plane 2	3.41E-07	6.23E-08	1.58E-07	1.74E-06	3.27E-07	1.09E-06	1.40E-06	2.65E-07	9.32E-07
	Plane 3	3.20E-07	6.14E-08	1.53E-07	1.59E-06	2.75E-07	1.01E-06	1.27E-06	2.14E-07	8.57E-07
	Plane 4	2.90E-07	5.59E-08	1.43E-07	1.48E-06	2.58E-07	9.62E-07	1.19E-06	2.02E-07	8.19E-07
	Plane 5	2.62E-07	4.48E-08	1.37E-07	1.23E-06	1.97E-07	8.10E-07	9.68E-07	1.52E-07	6.73E-07
	Plane 6	2.22E-07	3.11E-08	1.23E-07	8.73E-07	1.43E-07	5.91E-07	6.51E-07	1.12E-07	4.68E-07
	Plane 7	1.22E-07	1.86E-08	6.60E-08	4.57E-07	1.06E-07	2.87E-07	3.35E-07	8.74E-08	2.21E-07
	Plane 8	8.89E-08	1.52E-08	4.52E-08	3.11E-07	8.85E-08	1.61E-07	2.22E-07	7.33E-08	1.16E-07
	Plane 9	4.70E-08	9.72E-09	2.08E-08	1.52E-07	5.29E-08	9.72E-08	1.05E-07	4.32E-08	7.64E-08

Table 9. Changes in the average pressure, flow rate and total resistance during T0-T1 stages

	Before MARPE (T0)			After MARPE (T1)			ΔT1-T0			Percentage of change [(ΔT1-T0)/T0]x100		
	Max. Inspiration 1.080 s	Rest 1.730 s	Max. Expiration 2.805 s	Max. Inspiration 1.080 s	Rest 1.730 s	Max. Expiration 2.805 s	Max. Inspiration 1.080 s	Rest 1.730 s	Max. Expiration 2.805 s	Max. Inspiration 1.080 s	Rest 1.730 s	Max. Expiration 2.805 s
Average Pressure [Pa]	-69.2919	6.754787	38.9248	-30.8579	3.39817	18.46018	38.43398	-3.35662	-20.4646	-55.47	-49.69	-52.58
Flow rate [kg/s]	0.000684	0.000228	0.00106	0.000679	0.000179	0.000761	-0.000005	-0.000049	-0.000299	-0.73	-21.49	-28.21
Total Resistance [1/m·s]	-101304	29626.26	36721.51	-45446.1	18984.19	24257.79	55857.82	-10642.1	-12463.7	-55.14	-35.92	-33.94

Adopting the electric current formulation (R=V/I; V, voltage; I, current; R, resistance), the resistance can be calculated using an equation (R = P/Q; P, pressure; Q, quantity of fluid current; R, resistance)

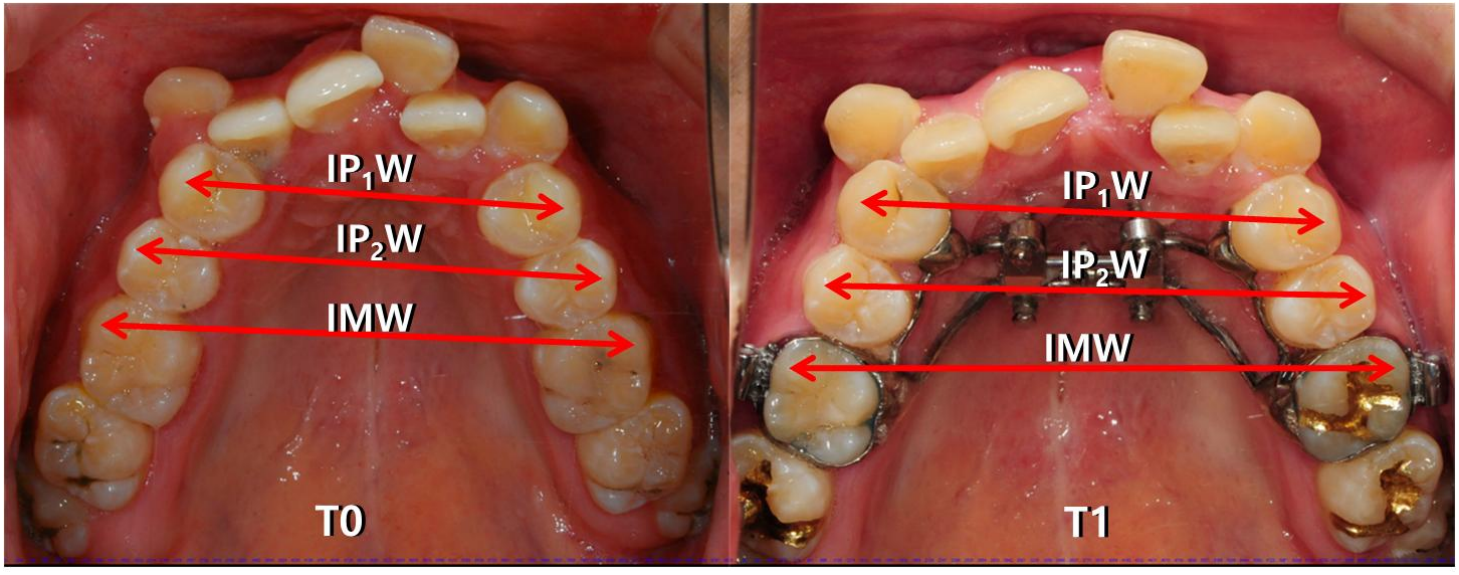

Fig. 1. Changes in maxillary dental arch width before (T0) and after (T1) MARPE. IP1W, inter-first premolar width; IP2W, inter-second premolar width; IMW, inter-first molar width.

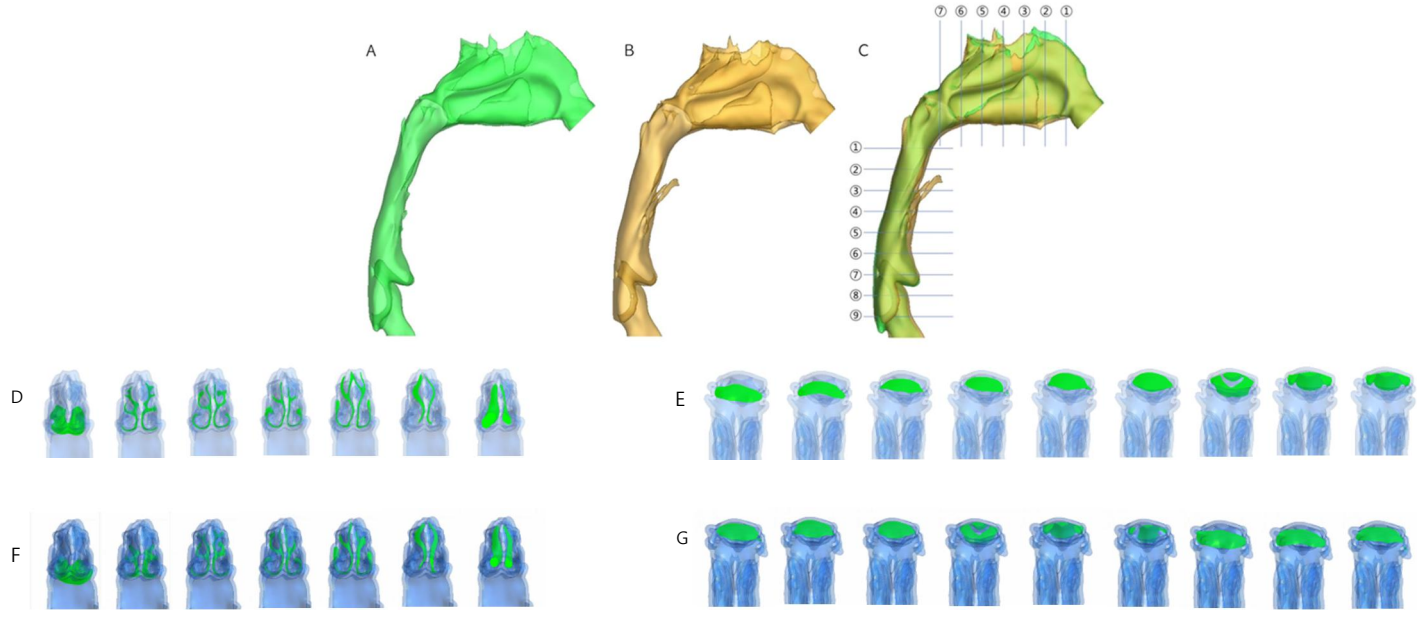

Fig. 2. Three-dimensional models of the upper airway. T0 (A, green), T1 (B, yellow) and superimposition (C) of the models showing the locations of seven planes in the nasal cavity and nine planes in the pharynx. The superimposition was performed with the best-fit method using the anterior cranial base of T0 and T1 models, making the other structures invisible, then showing the upper airway only. Comparison of the cross sectional airway area between T0 (D and E) and T1 (F and G) at sections from ① to ⑦ in nasal cavity (D and F, from left to right) and from ① to ⑨ in Pharynx (E and G, from left to right).

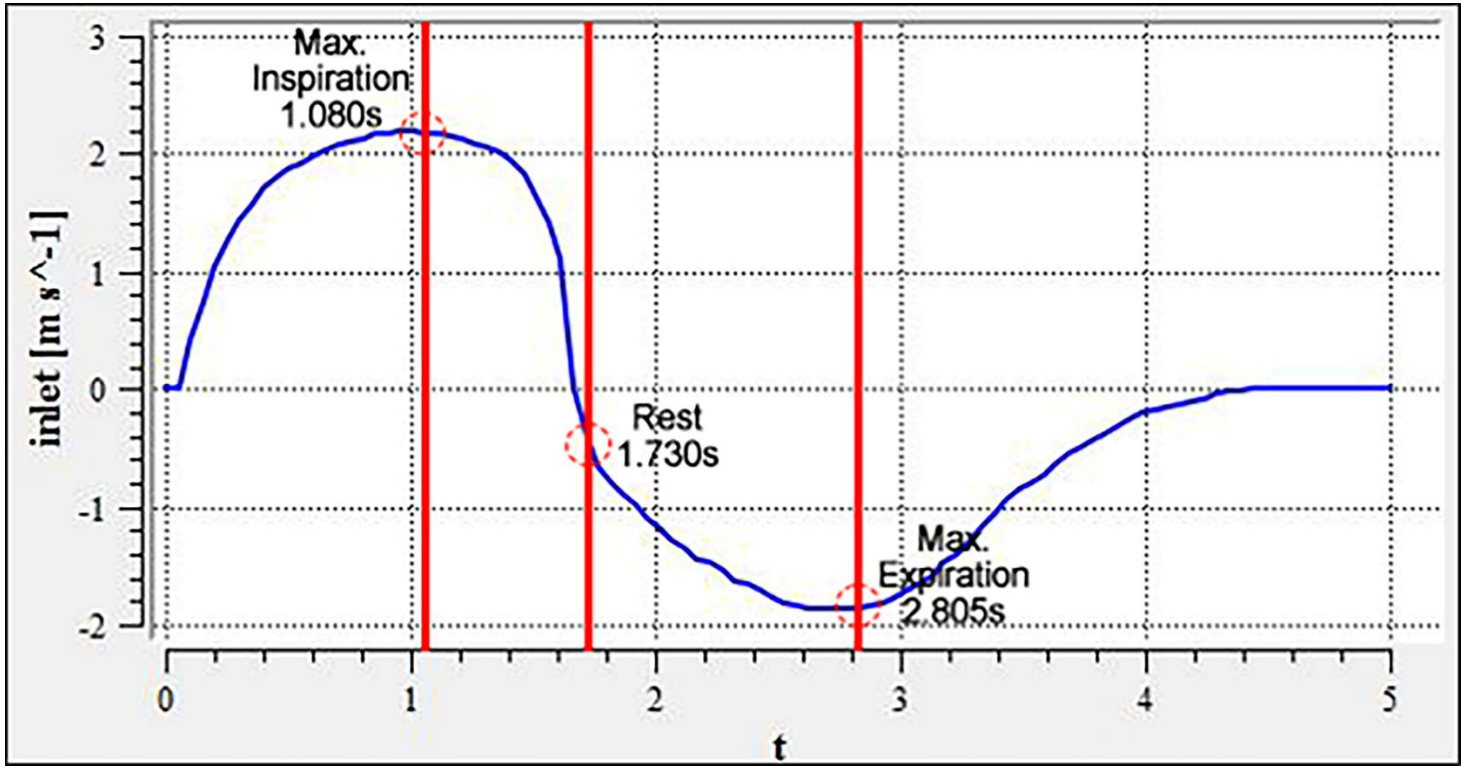

Fig. 3. Respiratory cycle used in the simulation. Total duration of one cycle, 5 seconds; maximum inspiration at 1.080 seconds; rest at 1.730 seconds; and maximum expiration at 2.805 seconds.

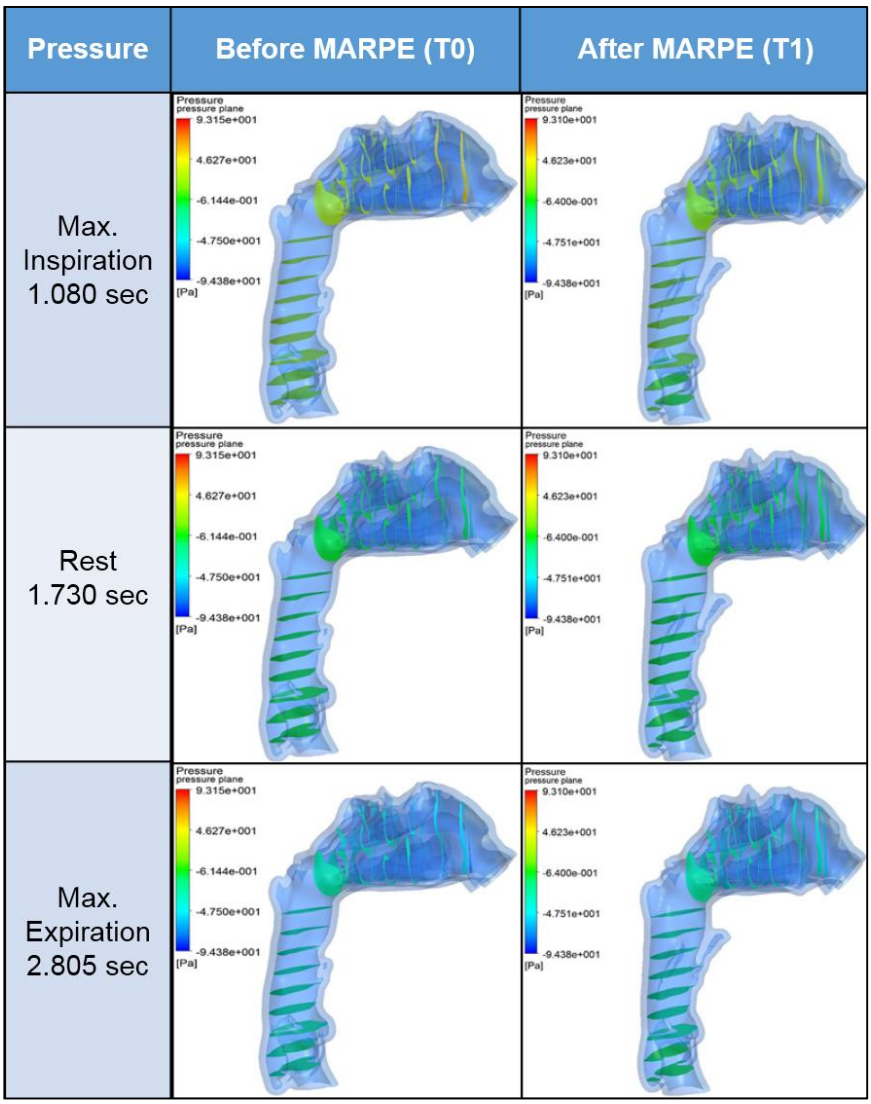

Fig. 4. Comparison of the airflow pressure in the nasal cavity and the pharynx during the respiratory cycle.

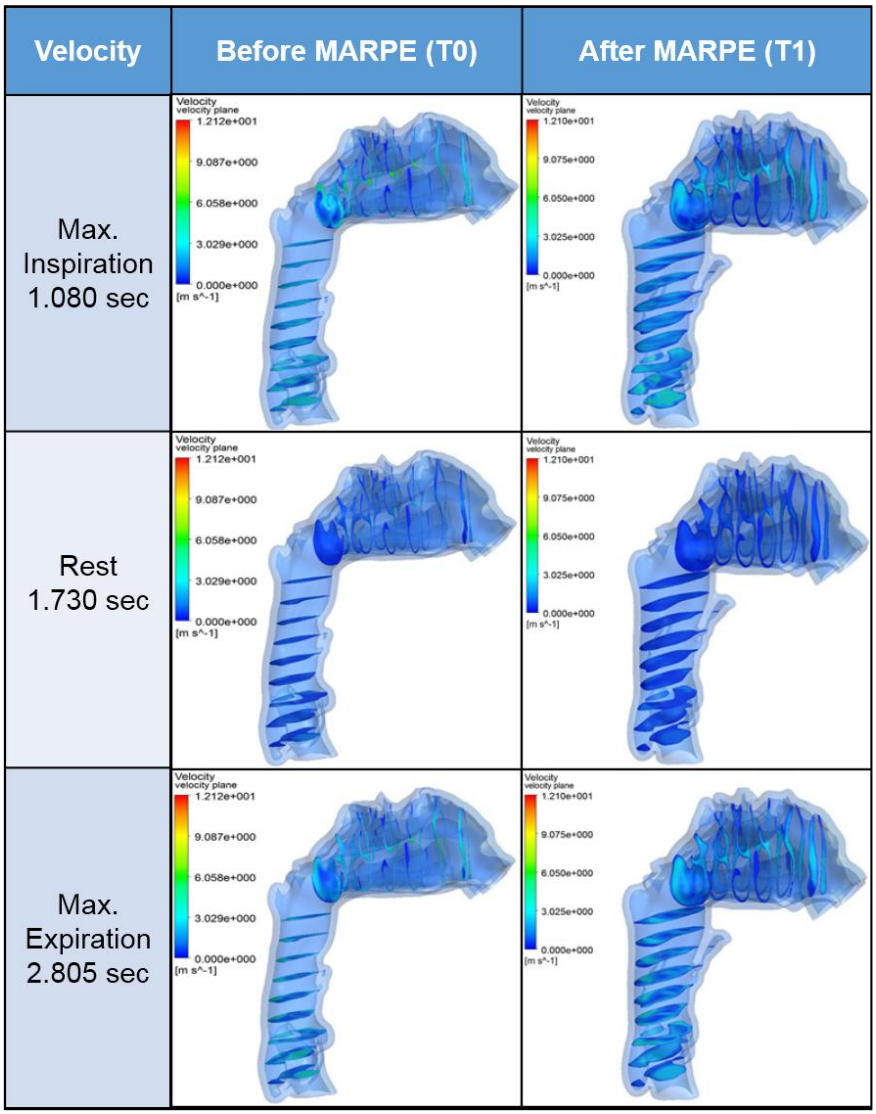

Fig. 5. Comparison of the airflow velocity in the nasal cavity and the pharynx during the respiratory cycle.

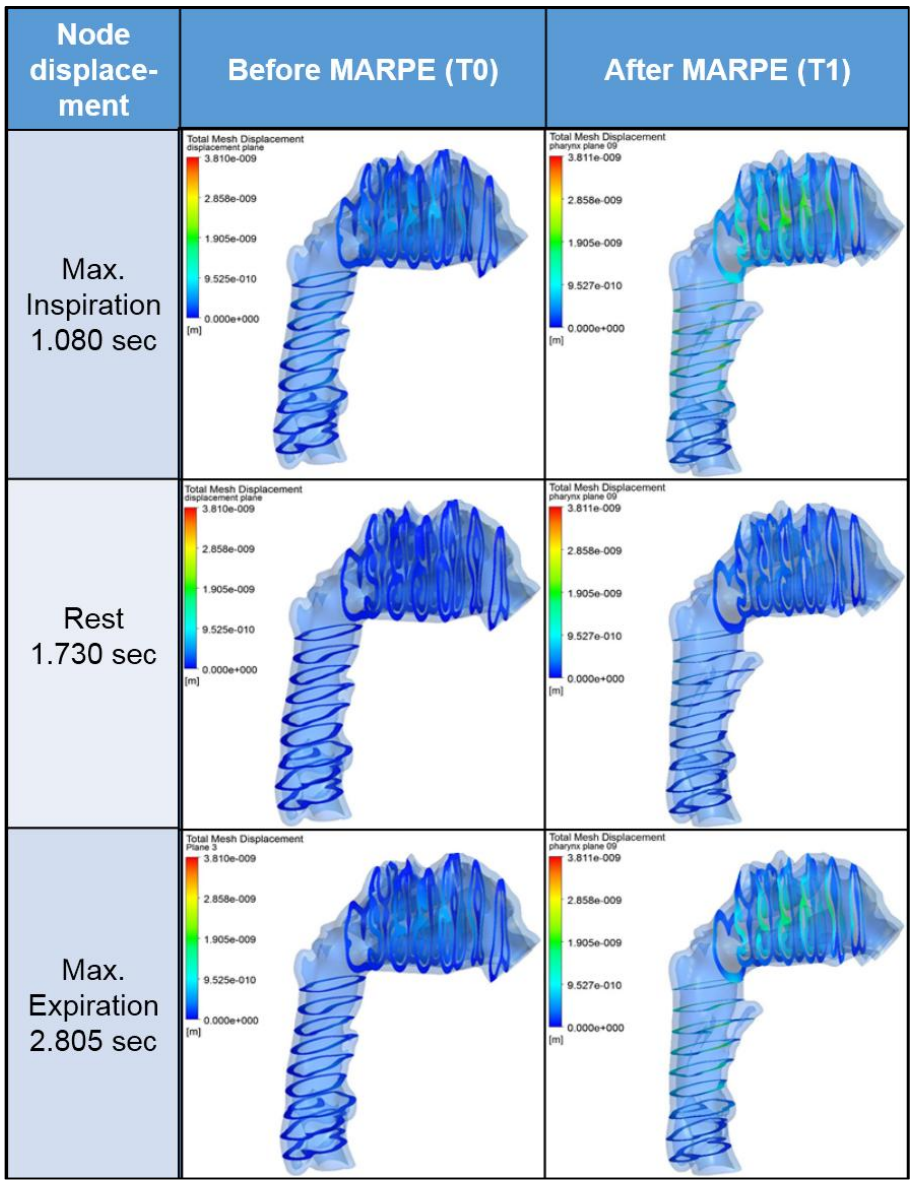

Fig. 6. Comparison of the node displacement in the soft tissue of the airway wall during the respiratory cycle.